ACCOUNTS
of chemical research

First-Principles Modeling of Dye-Sensitized Solar Cells: Challenges and Perspectives

FRéDéRIC LABAT, TANGUI LE BAHERS, ILARIA CIOFINI, AND CARLO ADAMO*

LECIME, Laboratoire d'Electrochimie, Chimie des Interfaces et Modélisation pour l'Energie, UMR 7575 CNRS, Ecole Nationale Supérieure de Chimie de Paris – Chimie ParisTech, 11 rue P. et M. Curie, 75231 Paris Cedex 05, France, and Institut Universitaire de France, 103 Boulevard Saint Michel, F-75005 Paris, France

RECEIVED ON DECEMBER 13, 2011

CONSPECTUS

Since dye-sensitized solar cells (DSSCs) appeared as a promising inexpensive alternative to the traditional silicon-based solar cells, DSSCs have attracted a considerable amount of experimental and theoretical interest. In contrast with silicon-based solar cells, DSSCs use different components for the light-harvesting and transport functions, which allow researchers to fine-tune each material and, under ideal conditions, to optimize their overall performance in assembled devices. Because of the variety of elementary components present in these cells and their multiple possible combinations, this task presents experimental challenges. The photoconversion efficiencies obtained up to this point are still low, despite the significant experimental efforts spent in their optimization.

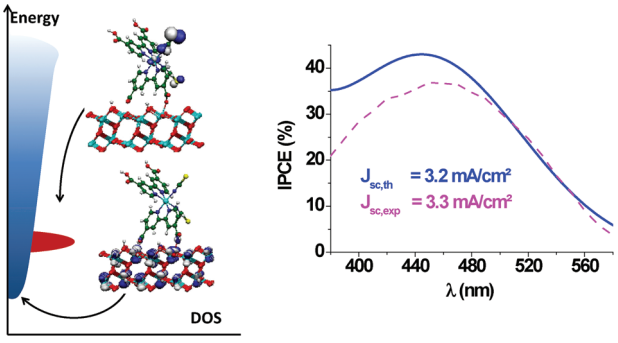

The development of a low-cost and efficient computational protocol that could qualitatively (or even quantitatively) identify the promising semiconductors, dyes, and electrolytes, as well as their assembly, could save substantial experimental time and resources. In this Account, we describe our computational approach that allows us to understand and predict the different elementary mechanisms involved in DSSC working principles. We use this computational framework to propose an in silico route for the ab initio design of these materials. Our approach relies on a unique density functional theory (DFT) based model, which allows for an accurate and balanced treatment of electronic and spectroscopic properties in different phases (such as gas, solution, or interfaces) and avoids or minimizes spurious computational effects.

Using this tool, we reproduced and predicted the properties of the isolated components of the DSSC assemblies. We accessed the microscopic measurable characteristics of the cells such as the short circuit current (J_{sc}) or the open circuit voltage (V_{oc}), which define the overall photoconversion efficiency of the cell. The absence of empirical or material-related parameters in our approach should allow for its wide application to the optimization of existing devices or the design of new ones.

1. Introduction

Production of energy from the sun with renewable material such as in dye-sensitized solar cells (DSSCs) has attracted a considerable amount of attention since O'Regan and Grätzel published their pioneering work in 1991.[1−3] Easily fabricated and low-cost, these devices paved the way to a new generation of economic photovoltaic modules, appearing as a promising alternative to silicon-based solar cells. Low costs and higher functionalities were essentially achieved by separating light harvesting and charge separation, as plants do in natural photosynthetic processes.

The working principle of a DSSC is schematically described in Figure 1. Light is harvested by a large surface area of dyes grafted on the surface of a wide bandgap semiconductor (such as TiO_2 or ZnO) in contact with an electrolyte (typically I_3^-/I^- in an organic solvent) and closed by a counter electrode, usually made of Pt. The elementary steps

Published on the Web 04/12/2012 www.pubs.acs.org/accounts
10.1021/ar200327w

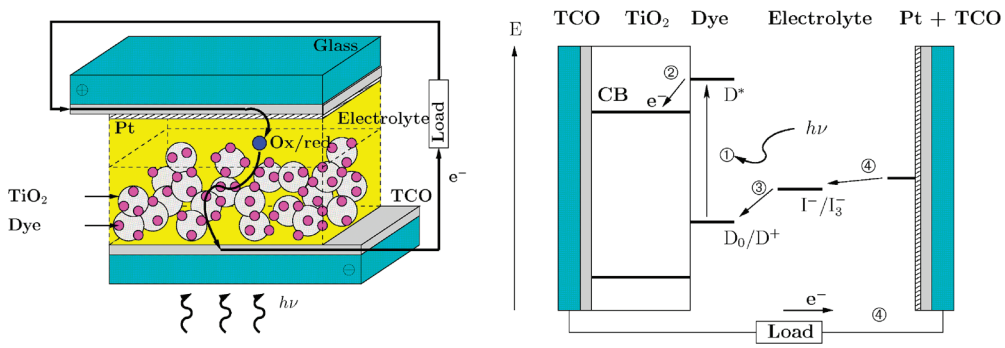

FIGURE 1. DSSC schematic (left) structure and (right) working principles. TCO stands for transparent conducting oxide.

involved can be thus represented as follows:

$$\text{dye} + h\nu \rightarrow \text{dye}^* \quad (1)$$

$$\text{dye}^* \rightarrow \text{dye}^+ + e_{\text{n-SC}}{}^- \quad (2)$$

$$2\text{dye}^+ + 3\text{I}^- \rightarrow 2\text{dye} + \text{I}_3{}^- \quad (3)$$

$$\text{I}_3{}^- + 2e_{\text{Pt}}{}^- \rightarrow 3\text{I}^- \quad (4)$$

Upon absorption of light in the visible−near-IR range, dye molecules, promoted in an electronically excited state (eq 1), inject electrons into the conduction band of the semiconductor (eq 2). Oxidized dyes are regenerated by a reducing agent of the electrolyte (usually I^-), thus converted to the corresponding oxidized species ($I_3{}^-$, eq 3). This latter is subsequently reduced at the counter-electrode (eq 4). The overall charge carrier motion gives rise to the macroscopic photocurrent. As a consequence of the photoinduced electron transfer from the dye to the semiconductor, the electronic density increases in the oxide, giving rise to an electrochemical potential difference (i.e., a voltage) between the semiconductor and the electrolyte.

The corresponding photoconversion efficiency, η, can be then defined as follows:

$$\eta = \frac{V_{\text{oc}} J_{\text{sc}} \text{FF}}{P_i} \quad (5)$$

where J_{sc} is the photocurrent density at short-circuit, V_{oc} the open-circuit photovoltage (see Figure 1), P_{i} the intensity of the incident light, and FF the fill factor. This latter is an important cell parameter that defines the ratio of the actual maximum obtainable power to the product of the open-circuit voltage and short-circuit current.

Unlike a standard silicon solar cell, in DSSCs, electrons and holes are transported in different media, thus allowing for both a separate optimization of each medium and an optimization of the charge extraction at each interface.

Up to now, intensive research has been performed to increase the photoconversion efficiency, reaching values higher than 10% for titania-based solar cells sensitized with ruthenium complexes (e.g., N719)[4] and organic dyes.[5] Nevertheless, performances are leveling off, as suggested by a recent publication[6] showing that devices belonging to the N719/TiO_2 family have almost reached their maximum efficiency.

Higher performances are expected to be achievable as long as the full design of new components (dyes, oxide, and redox couple), as well as their optimal assembly, is considered. Given the great variety of elementary components in these cells and their multiple possible combinations however, this task is still extremely challenging. Developing a low-cost and efficient computational protocol able to qualitatively (or even quantitatively) identify the promising semiconductors, dyes, and electrolytes, as well as their assembly, which could efficiently generate a photocurrent, would thus allow one to drive experiments through an efficient *in silico* prescreening of all different basic components of DSSCs and therefore offer substantial time and resource savings at the experimental level. Not surprisingly many computational studies were devoted to the characterization of single components and interfaces of DSSCs.[7,8]

In this Account, we report on a recently developed computational protocol enabling understanding and prediction of the elementary steps involved in DSSC working principles. The core of our approach relies on a unique density functional theory (DFT)-model, which allows for an accurate and balanced treatment of electronic and spectroscopic properties in different phases (gas, solution, or interfaces), thus avoiding (or at least minimizing) spurious computational effects, related to both models and methods applied.

After a concise description of the computational protocol (section 2), the results obtained on individual components

and their interplay for existing DSSCs are collected in section 3 while in section 4 is reported an example of *in silico* design of new DSSCs.

2. The Computational Protocol

Modeling the main steps involved in a DSSC requires one to model electron transfer phenomena, making an explicit treatment of electrons by a proper quantum chemical treatment mandatory. In addition, in order to set up an approach to screen novel candidates, any method introducing empirical parameters not straightforwardly extendable to novel materials has to be excluded.

Considering the high complexity of the systems to be modeled, DFT-based methods appear as a natural choice due to their appealing performance to accuracy ratio.

Nowadays, DFT is probably the most widely used method in computational chemistry, yielding an accurate prediction of several ground asnd excited state properties.[9] Its success is mainly related to the recent development of a wide variety of increasingly complex and accurate exchange–correlation functionals. Among these, the so-called hybrid functionals, which explicitly include a fraction of Hartree–Fock (HF) exchange, are probably the most popular, at least for molecular systems. Global hybrids (GH), such as B3LYP[10] or PBE0,[11] actually emerged as the most applied in chemistry. Although the better performance of hybrid functionals with respect to semilocal ones still holds for extended systems, especially as it concerns band gaps, hybrids still remain not so largely used for solids, since the evaluation of the exact HF exchange contribution at long range is computationally demanding when plane waves are considered as basis sets.[12] When localized (Gaussian) basis sets are chosen however, hybrid functionals can be efficiently applied to periodic systems.[13,14]

The same GHs (such as PBE0[9]) were proven to yield impressive performances for studying excited state properties of molecular systems at time-dependent DFT level. In some delicate cases however, a correction of the exchange potential form to obtain the correct long-range behavior is required and obtained through the use of range-separated hybrids (RSH). These functionals (see, for instance, ref 15) have been shown as particularly adapted when dealing with through-space charge-transfer transitions, for which standard GHs fail to accurately reproduce the experimental data[9] with the exception of latest generation functionals of the Minnesota family, such as M06-2X and M08-HX, which actually perform better than the RSH (CAM-B3LYP) for the description of charge transfer excitations with intermediate spatial overlap.[15]

As a trade-off, GHs (such as PBE0) appear as a good compromise for a consistent description of both ground and excited state properties of molecules, surfaces, and solids, as needed to model DSSCs, without introducing any empirical and material-dependent parameter.

At the same time, environmental effects on the electronic properties should be taken into account. Although the effect of the solvent highly depends both on its nature and on that of the transitions involved,[9] solvation can be routinely taken into account at reasonable computational cost by considering implicit solvation models such as polarizable continuum models (PCM, see ref 16a for an overview and ref 16b for the latest developments for solvation effects on spectroscopy). In such a case, the solvent is modeled by a (continuum) medium characterized by a static dielectric constant, polarizing the solute and polarized by the solute. Eventually, specific bonding interactions between the solute and the solvent can also be addressed by mixed explicit/implicit models, explicitly including the first solvation shell in the electronic calculation and embedding the resulting cluster in a PCM to simulate the bulk solvent effects. Surface interactions could be also considered as a particular case of environmental effects, significantly tuning the spectral properties of dyes. An inexpensive yet powerful tool to include such effects combines the ONIOM method[17] with electronic embedding (EE) potentials.[18] The wave function of the chemically relevant part of the system can be polarized by the electrostatic contribution of its surroundings, by an appropriate division of all subparts of the system.

Finally, since several competing kinetic processes are involved in DSSCs, a simple method to evaluate the electron injection times is also required. To this end, the injection time (τ) was estimated from the energetic broadening (Δ) of the donor orbital of the dye upon adsorption, using a model derived from the Newns–Anderson approach,[19] as follows:

$$\tau = C/\Delta \tag{6}$$

C being a constant (658 fs meV).

Overall, our computational protocol is based on the use of DFT in conjunction with a GH (PBE0) to study both isolated and extended systems (i.e., 2D or 3D periodic systems), properly including the most relevant environmental effects (solvation, embedding).

3. Insights on Individual Components and on Their Interplay

In order to enhance the performance of DSSCs, a common strategy applied at the experimental level relies on an initial

optimization of their isolated components (dye, semiconductor, or electrolyte), followed by a deep analysis and tuning of their assembly. Following this line, at the theoretical level, the structural and electronic features of the isolated dyes and semiconductors can be first analyzed to prescreen and optimize suitable candidates for efficient devices.

3.1. Isolated Components. The main electronic requirement for semiconductors to be used for DSSC applications is related to the position of the band edges. In particular, a material transparent to UV−vis radiation with a conduction band edge below the energy of the excited state of the dye (D*, Figure 1) is desired.

From our studies[20−23] and those of others,[12,23] it appears that GHs and periodic boundary conditions (PBCs) yield an accurate description of both geometric and electronic structures of bulk and surfaces of semiconductors commonly involved in DSSC devices (i.e., TiO_2 or ZnO). Indeed, local functionals generally show a systematic and problematic underestimation of the semiconductor band, as reported in Table 1 for TiO_2 and ZnO, for instance.

TABLE 1. Computed and Experimental Gaps (in eV) for TiO_2 and ZnO

	LDA	PBE	PBE0	exptl
TiO_2 (anatase)[a]	2.33	2.36	4.50	3.18[c]
ZnO (wurtzite)[b]	1.46	1.46	3.93	3.44[d]

[a]Reference 20. [b]Reference 22. [c]See ref 28 of ref 20. [d]See ref 33 of ref 21.

For the sake of completeness, it should be mentioned that a specifically developed RSH functional[24] performs better than popular GHs for the band gap determination. Nevertheless, the performance of HSE for the description for excited states is expected to be rather poor and thus unsuitable for DSSCs modeling, where an accurate description of both the semiconductor and the dye excited state properties are needed.

Concerning dyes, the best photoconversion efficiencies are obtained with ruthenium- and osmium-based dyes for TiO_2-based cells, while organic dyes such as eosin-Y and indolines (D131, D102, and D149, Figure 2) are common dyes used in ZnO-based cells, especially due to their low costs. Most of the organic dyes used are generally "push−pull" architectures made of the covalent assembly of (i) an electron-donating group (D) and (ii) an electron-withdrawing (A) group. In this case, the excited state responsible for the injection into the conduction band of the semiconductor is generated by a charge transfer (CT) transition from the donor to the acceptor group. On the other hand, in the case of Ru or Os complexes the excited state basically corresponds to a metal-to-ligand CT transition. In both

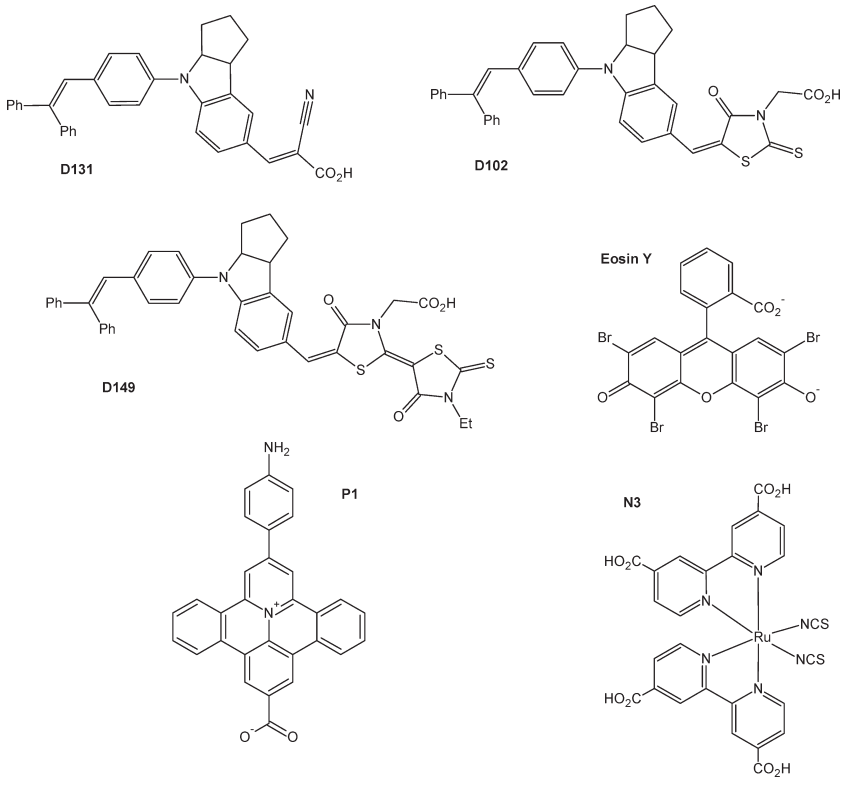

FIGURE 2. Structures of selected dyes.

cases, the dye is chemically linked to the surface via an anchoring group.

We have demonstrated that the electronic properties of the isolated dyes as well as their absorption spectra can be very accurately described using a GH such as PBE0, especially when properly taking into account solvent effects using a PCM approach.[9,25−29] The charge transfer length and character associated with a given electronic transition can be further qualitatively analyzed by considering a charge transfer index (d_{CT}), recently developed in our group.[30]

On this basis, some intrinsic structural and electronic properties required (but not sufficient) for a dye to generate a photocurrent upon adsorption on an oxide surface can be defined and computed:

- the anchoring group should be positioned on the electron-accepting group
- the HOMO and LUMO of the dye should be energetically computed above the valence band edge (VBE) and the conduction band edge (CBE) of the oxide, respectively
- the absorption spectrum should significantly overlap with the solar spectrum
- the transition involved in the photoconversion phenomenon should have a high intensity
- the fluorescence lifetime should be sufficiently high (above the nanosecond time scale) to allow an electronic injection to the semiconductor from the excited state of the dye before quenching of the excited state by a radiative decay

As an example, all of the above-mentioned parameters were computed for a dye belonging to a new family characterized by the presence of a polycyclic pyridinium ring as electron-withdrawing group (P1, Figure 2).[31] The first transition is computed (and experimentally measured) around 450 nm, thus having a good overlap with the solar spectrum. The variation of electronic density (Figure 3) from the ground to the excited state associated with this transition qualitatively indicates its charge transfer character. This is quantitatively confirmed by a computed charge transfer length of 4.1 Å. The anchoring carboxylate group is linked to a pyridinium polycyclic fragment (i.e., the acceptor group), which will facilitate the electronic injection upon illumination of the dye. Finally, the computed LUMO level is found 0.22 eV above the CBE computed on a pure $(10\bar{1}0)$ surface of ZnO. Consequently, this dye fulfills all requirements needed to be successfully used in ZnO-based DSSCs.

3.2. Interfaces. In order to allow an efficient injection from the dye to the semiconductor, the molecule should

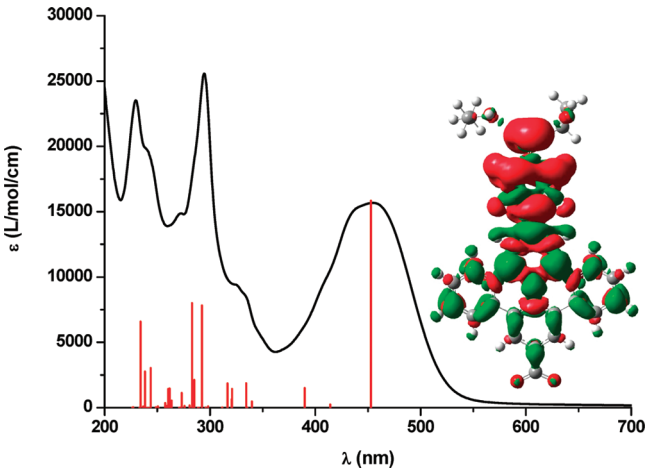

FIGURE 3. Experimental UV−vis spectrum (black) and computed vertical electronic transitions (TD-DFT/PBE0/6-31++G(d,p), red) along with the computed difference in density between the first excited state and the ground state (green and red refer to an increase and a decrease of electronic density, respectively; isovalue 0.0005 au).

firmly adsorb on the semiconductor to avoid desorption phenomena. An efficient modeling protocol should thus also be able to predict the energetic and structural features related to this adsorption process.

Different anchoring groups can be used to chemically link the dyes to the semiconductor, the most common being a carboxylic moiety. Nevertheless, since in most cases the anchoring group is electronically and geometrically decoupled from the rest of the dye, model systems containing only the relevant anchoring group and the semiconductor can be used to screen different adsorption modes of the dye on the surface at low computational cost.

This strategy has been applied to N3/TiO_2 and Eosin-Y/ZnO, prototypical examples of DSSCs. For the N3/TiO_2 system, the bi-isonicotinic acid (BINA) molecule over an anatase (101) surface was considered,[32] while for the EY/ZnO DSSC a formic acid over a wurtzite $(10\bar{1}0)$ surface was studied.[22] Both anchoring groups were found to adsorb in a dissociative way, with a preferred bidentate binding mode for formic acid and a mixed bidentate/monodentate one for BINA.

The same procedure was recently applied to propose and study new anchoring groups based on acetylacetone[33,34] and catechol[34] derivatives (Supporting Information) particularly tailored for ZnO-based applications due to their low acidity. These studies confirmed not only that all these groups efficiently anchor the dye to the surface but also that in the case of acetylacetone ATR-IR experimental spectra can be predicted and experimentally used to follow the adsorption process.[33,34]

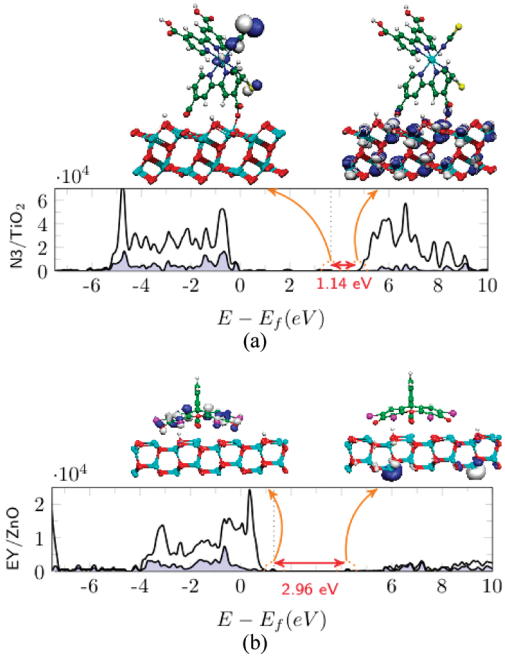

FIGURE 4. Computed densities of states and relevant Γ-point frontier crystalline orbitals of the (a) N3/TiO_2 (HOMO and LUMO) and (b) EY/ZnO (HOMO and LUMO+2) systems. Isovalues: |0.040| a.u. for HOMO, |0.007| a.u. for LUMO, and |0.020| a.u. for LUMO+2.

The adsorption geometry obtained by the study of the model systems can next be used as starting point to model the real dye/semiconductor interface always using PBC.

In such a way, the adsorption of N3 on anatase (101)[35] as well as EY on wurtzite[36] was recently investigated. Analogously to the BINA, N3 adsorbs in a mixed bidentate/monodentate fashion, while EY binds both through its carboxylic acid moiety and its xanthene, displaying surface coordination with both O and Br atoms (Supporting Information). Computed densities of states (DOS) of both systems, as well as relevant frontier crystalline orbitals, are presented in Figure 4. Clearly, two opposite situations appear. The electronic structure of N3/TiO_2 is compatible with an electron injection from the dye to the semiconductor, with HOMO and LUMO localized on the former and the latter, respectively. On the other hand, the EY/ZnO one is not, since the HOMO is localized on the dye and only the LUMO+2 is exclusively localized on the semiconductor.

Further qualitative insights on the nature of the first excited state of such systems were obtained, in analogy to spectroelectrochemistry experiments, by considering the electronic structure of the reduced systems. Plotting spin maps thus reveals the feasibility of the electron injection (Supporting Information). It is clear that upon addition of one electron, injection is observed in the case of N3/TiO_2 while the extra electron still remains mostly localized on the dye in the EY/ZnO assembly. Addition of a second electron in this latter case however leads to an equal repartition of the spin density between the substrate and the adsorbate, thus pointing out that to inject one electron to the substrate, two electrons might be involved. Monophotonic and biphotonic processes might thus rule the N3/TiO_2 and EY/ZnO operations, respectively, explaining the larger photoconversion efficiency observed for the first system.

Using eq 6, electron injection times were computed to be 2, 22, and 8 fs for the BINA/TiO_2, N3/TiO_2 and EY/ZnO]$^-$ systems, respectively. These values are in fair agreement with available experimental data ranging between 3 and 6.5 fs for BINA/TiO_2, and 30 and 50 fs for N3/TiO_2 (see ref 35 and references therein), further underlying the level of accuracy of the calculations.

Finally, the effect of the adsorption on the spectral features can also be evaluated. If, in agreement with the experimental data,[37] the adsorption on TiO_2 only slightly modifies the spectral properties of N3 (Figure 5), more marked effects can be noticed for EY/ZnO. In particular, the relative intensities of the two main bands can only be reproduced when taking into account electrostatic effects (ONIOM+EE case) due to the presence of the semiconductor.

Since the semiconductor surface is exposed to the electrolyte, the effect of the coadsorption of its molecules on the electronic structure of the semiconductor should also be addressed. Using the same protocol employed for the adsorption of the anchoring groups and dyes on the surfaces, we investigated the influence of the electrolyte composition on the open-circuit voltage (V_{oc}) of the DSSC,[38] a key parameter of the cell directly related to the photoconversion efficiency (eq 5). Since V_{oc} is related to the difference between the quasi-Fermi level of the semiconductor and the electrochemical potential of the redox couple of the electrolyte (eq 7),[38] it is directly related to the CBE position (eq 8). In particular, the higher the CBE energy, the higher the V_{oc}.

$$qV_{oc} = \varepsilon_{F,n} - \mu_{redox} \tag{7}$$

$$\varepsilon_{F,n} = E_{CBE} + kT \ln\left(\frac{n_c}{N_c}\right) \tag{8}$$

To assess the effect of the electrolyte molecules on the CBE energy pointed out at the experimental level, three molecules usually used as solvent (nitromethane (NM), acetonitrile (AN), and dimethylformamide, (DMF)) were adsorbed on a (10$\bar{1}$0) ZnO surface. The influence of a common additive, 4-*tert*-butylpyridine (TBP, modeled as methylpyridine) was also

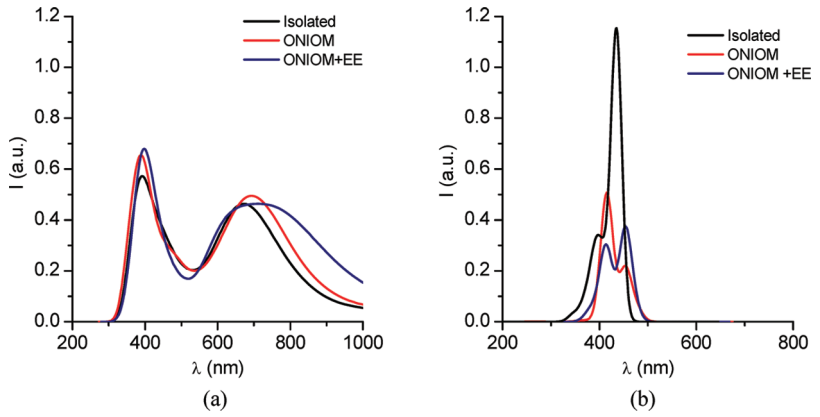

FIGURE 5. Simulated UV−visible absorption spectra of (a) N3/TiO_2 and (b) EY/ZnO.

considered. The theoretical results were compared with experimental measurements of V_{oc} of ZnO/D149-based DSSCs built and characterized experimentally using these different molecules as solvent or additives. An experimental increase of V_{oc} in the order NM < AN < DMF ≈ TBP was outlined in qualitative agreement with the computed CBE variation (Figure 6). The slight discrepancy observed for DMF and TBP could be ascribed to a variation of the redox potential ($E°$) of I_3^-/I^- (also ruling the V_{oc}, eq 5) in the different media.[38]

4. *In Silico* Design of New Systems: From Single Components to Cell Characteristics

Studies reported above showed that the computational protocol used for investigating both molecules and adsorbed molecules on oxide surfaces is reliable and can yield useful insights on existing devices. It is now possible to go beyond the explanation of experimental observation and to use *in silico* experiments to design new single components (dyes, anchoring groups, electrolyte component) and, overall, new cell assemblies.

Let us consider again the organic dye P1 (Figure 2), whose isolated properties were presented in section 3, in order to predict its ability to generate a photocurrent upon adsorption on ZnO (10$\bar{1}$0) surface.[31] To that purpose, with the same protocol as for the adsorption of the anchoring group and the electrolyte's molecules, we adsorbed the P1 dye on a ZnO (10$\bar{1}$0) surface. Passivation of the surface was also taken into account and simulated by adsorption of water molecules to ensure reasonable computational costs. Figure 7 presents the optimized structure of this system and the computed DOS. In the present case, both the HOMO and the LUMO of the dye lie below the VB and CB edges of the semiconductor, respectively. In particular, the calculated energy difference between the CB bottom edge of ZnO and

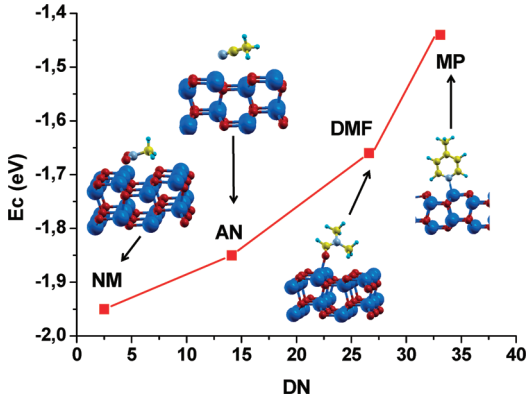

FIGURE 6. CBE energy (and structures) of systems containing molecules adsorbed on a ZnO(10$\bar{1}$0) surface.

the LUMO of P1 is ca. 0.58 eV, notably different from the configuration derived from calculations on isolated species (see section 3). We should note that (i) the oxidation potential is not a localized level but a large band and (ii) the computed CBE energy does not take into account the entropy of the injected electron, which is known to be high;[2] a non-negligible overlap between the LUMO and the CB edge that may permit electron injection might exist in the real device. Nevertheless, with such an orbital configuration, the injection rate is expected to be low, and this case outlines that contrary to the molecular approach used for studying properties of the isolated dye, only the periodic calculations explicitly integrating both the ZnO surface and the dye allows one to predict (and show) that ZnO sensitized by P1 should have a low efficiency due to an unfavorable electronic structure for electron injection.

To enhance device performances, the CBE position can be tuned by modifying the electrolyte composition, as reported in the previous section. We determined the influence of such molecules on the electronic structure of the P1/ZnO surface

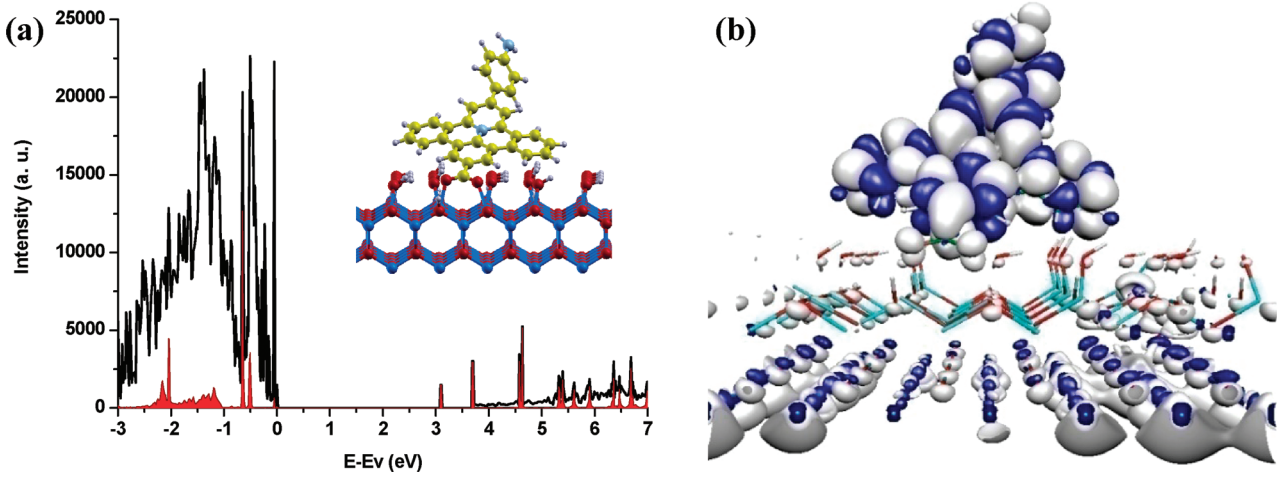

FIGURE 7. (a) Computed structure for the P1 dye adsorbed on the water passivated (10$\bar{1}$0) ZnO surface along with its total (black) and projected on the dye (red) DOS. (b) Spin density of reduced system P1/ZnO in presence of Li^+.

by coadsorbing lithium ion (Li^+) or methylpyridine (MP), two common additives well-known for downshifting and upshifting the CBE level, respectively. From our calculations, although the LUMO of the system still remains below the CB bottom edge, adsorption of Li^+ sizably decreases the gap between the LUMO and the CB edge by ca. 0.45 eV (from 0.58 to 0.12 eV). On the other hand, the MP molecule increases this energy gap from 0.58 to 0.74 eV, predicting that these additive molecules should substantially influence the electron injection, albeit in opposite directions.

The electron injection of the three systems (P1/ZnO, (P1+Li^+)/ZnO, and (P1+MP)/ZnO) was also theoretically assessed analyzing the corresponding one-electron reduced systems, analogously to the N3/TiO_2 and EY/ZnO cases (section 3). Computed spin densities of the three above-mentioned systems are reported in Figure 7b and Figure SI.4, Supporting Information. In all cases, the spin densities are delocalized over both the dye and the ZnO surface. Without additive molecules in the electrolyte, the fraction of injected electrons into the semiconductor is 18%. With adsorbed Li^+, it increases to 43%, while with MP, a reduction of the injection to 9% is calculated. Consequently, based on these theoretical outcomes, it is clear that lithium ions should be added to the electrolyte to achieve higher efficiency.

Finally, it is also possible to simulate the incident photon to electron conversion efficiency (IPCE), widely used experimentally for characterizing solar cells. Integration of the IPCE curves, following eq 9, leads to the photocurrent of the system (J_{sc}), experimentally measured from the $J-V$ characteristics.

$$J_{sc} = \frac{e}{hc}\int \mathrm{IPCE}(\lambda)\lambda\phi_{\mathrm{AM1.5}}(\lambda)\,\mathrm{d}\lambda \qquad (9)$$

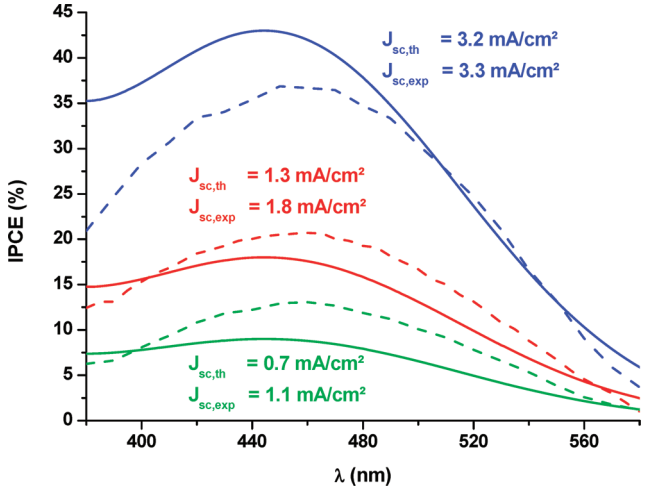

FIGURE 8. Experimental (dashed lines) and simulated (full lines) IPCE characteristics along with integrated current. Red lines correspond to an electrolyte without additives, blue line to an electrolyte containing Li^+, and green lines to an electrolyte containing a pyridine derivative.

This is done by first convoluting the UV−vis spectra of the dye computed at the TD-DFT level and imposing a maximum intensity proportional to the injection efficiency obtained from the spin density calculations. The simulated IPCE spectra so obtained are reported in Figure 8 in the case of the P1/ZnO system in comparison with the experimental data. From this figure, it is clear that the computational protocol here applied can be successfully used to tune the efficiency of the cells and predict the change in photoconversion efficiency in the presence of additives. Overall these results confirm the possibility of using *ab initio* calculations in order to rationalize and help the experimental optimization of the DSSCs.

5. Conclusions and Perspectives

The recent advances in DFT and TD-DFT methods allow nowadays for a good description and prediction of properties of the isolated components and assemblies that constitute the basic elements of DSSCs. Indeed, in order to get meaningful results, it is compulsory to use a level of theory adequate to treat on the same foot all components involved in the processes. This translates to the necessity of using at least a global hybrid functional for the description of their electronic structure. Furthermore, in order to avoid confinement effects, for the treatment of the dye−semiconductor interfaces a periodic approach seems to be the most reliable. Using such tools, we demonstrated that it is now possible not only to access miscroscopic quantities but also global measurable observables such as J_{sc} and V_{oc}, defining the overall photoconversion efficiency.

It also seems clear that the electrolyte plays a relevant role in DSSCs, and the first steps toward its explicit modeling were performed.

If the present computational approach has already proven its ability for interpretation and design of new cells, it is indeed important to stress that enhancements are still needed especially to provide a more realistic picture of the microscopic structure of the semiconductor and of the bulk electrolyte properties.

The authors are in debt for fruitful discussions and long-standing collaborations to Dr. P. P. Lainé (Université Paris Diderot) and Dr. T. Pauporté (ENSCP). M. Frisch and H. Hratchian (Gaussian Inc.), as well as K. Raghavachari (Indiana University), are also acknowledged. I.C. thanks the French National Agency for Research (ANR) for financial support in the framework of the program 2008 "Habitat intelligent et solaire Photovoltaïque" (Habisol) project ASYSCOL.

Supporting Information. Complete ref 14, schematic drawing of different anchoring groups, optimized N3/TiO_2 and EY/ZnO structures, and spin density computed for monoreduced N3/TiO_2, EY/ZnO, and P1/ZnO systems. This information is available free of charge via the Internet at http://pubs.acs.org.

BIOGRAPHICAL INFORMATION

Frédéric Labat was born in Pau (France) in 1980. He graduated from Chimie-Paristech (France) in 2004, where he also got a Ph.D. in Theoretical Chemistry in 2007. After a one-year stay at Université de Pau (France) as temporary assistant professor in 2008, he came back to Chimie-Paristech (France) first as a postdoctoral fellow and then as temporary assistant professor. Since 2010, he has a permanent position there as Maître de Conférences (assistant professor). His main research interests concern the application of DFT to solid-state systems, with a particular emphasis on DSSCs.

Tangui Le Bahers was born in Plésidy (France) in 1985. He graduated from Chimie-Paristech (France) where he got a Ph.D in Physical Chemistry in 2011. Currently, he is postdoctoral fellow at Rhodia in Paris (France). His main research interests are related to the photovoltaic devices, hybrid systems, and photochemistry.

Ilaria Ciofini was born in Arezzo (Italy) in 1973. After a degree in Chemistry at the University of Florence (Italy), she got a Ph.D. in Theoretical Chemistry in 2001 at University of Fribourg (Switzerland). After one year as postdoctoral fellow at the University of Wurzburg (Germany) and two years as associate CNRS researcher at Chimie-Paristech (Paris, France), she got a permanent CNRS position (in 2004). From 2010, she is Directeur de Recherche CNRS. Her main research interests are related to development and application of DFT and TD-DFT methods to magnetic and spectroscopic properties.

Carlo Adamo was born in Naples (Italy) in 1963 where he attended the University Federico II, receiving a Ph.D. in Theoretical Chemistry in 1995. Between 1993 and 2000, he was Assistant Professor at the University of Basilicata (Italy). In 2000, he moved to Chimie-ParisTech (France) as Associate Professor and became Full Professor in Theoretical Chemistry in 2004. In 2011, he was admitted to the Institute Universitaire de France as senior professor. His main research interests concern the development of DFT approaches and their applications in the field of energy production.

FOOTNOTES

*Corresponding author. E-mail: carlo-adamo@chimie-paristech.fr.
The authors declare no competing financial interest.

REFERENCES

1 O'Regan, B.; Grätzel, M. A low-cost, high-efficiency solar cell based on dye-sensitized colloidal TiO_2 films. *Nature* **1991**, *353*, 737–740.
2 Hagfeldt, A.; Boschloo, G.; Sun, L.; Kloo, L.; Pettersson, H. Dye-sensitized solar cells. *Chem. Rev.* **2010**, *110*, 6595–6663.
3 Spitler, M. T.; Parkinson, B. A. Dye sensitization of single crystal semiconductor electrodes. *Acc. Chem. Res.* **2009**, *42*, 2017–2029.
4 Yu, Q.; Wang, Y.; Yi, Z.; Zu, N.; Zhang, J.; Zhang, M.; Wang, P. High-efficiency dye-sensitized solar cells: The influence of lithium ions on exciton dissociation, charge recombination, and surface states. *ACS Nano* **2010**, *4*, 6032–6038.
5 Zeng, W.; Caot, Y.; Bai, Y.; Wang, Y.; Shi, Y.; Zhang, M.; Wang, F.; Pan, C.; Wang, P. Efficient dye-sensitized solar cells with an organic photosensitizer featuring orderly conjugated ethylenedioxythiophene and dithienosilole blocks. *Chem. Mater.* **2010**, *22*, 1915–1925.
6 Snaith, H. J. Estimating the maximum attainable efficiency in dye-sensitized solar cells. *Adv. Funct. Mater.* **2010**, *20*, 13–19.
7 (a) De Angelis, F.; Fantacci, S.; Selloni, A.; Grätzel, M.; Nazeeruddin, M. K. Influence of sensitizer's dipole on open-circuit potential of the dye-sensitized solar cell. *Nano Lett.* **2007**, *7*, 3189–3195. (b) Chen, P.; Yum, J. H.; De Angelis, F.; Mosconi, E.; Fantacci, S.; Moon, S.-J.; Baker, R. H.; Ko, J.; Nazeeruddin, Md. K.; Grätzel, M. High open-circuit voltage solid-state dye-sensitized solar cells with organic dye. *Nano Lett.* **2009**, *9*, 2487–2492.
8 Martsinovich, N.; Troisi, A. Theoretical studies of dye-sensitised solar cells: From electronic structure to elementary processes. *Energy Environ. Sci.* **2011**, *4*, 4473–4495.
9 Jacquemin, D.; Perpète, E. A.; Ciofini, I.; Adamo, C. Accurate simulation of optical properties in dyes. *Acc. Chem. Res.* **2009**, *42*, 326–334.
10 Becke, A. D. Density-functional thermochemistry. III. The role of exact exchange. *J. Chem. Phys.* **1993**, *98*, 5648–5652.

11 Adamo, C.; Barone, V. Toward reliable density functional methods without adjustable parameters: The PBE0 model. *J. Chem. Phys.* **1999**, *110*, 6158–6169.

12 Marsman, M.; Paier, J.; Stroppa, A; Kresse, G. Hybrid functionals applied to extended systems. *J. Phys.: Condens. Matter* **2008**, *20*, No. 064201.

13 Dovesi, R.; Saunders, V. R.; Roetti, C.; Orlando, R.; Zicovich-Wilson, C. M.; Pascale, F.; Civalleri, B.; Doll, K.; Harrison, N. M.; Bush, I. J.; D'Arco, Ph.; Llunell, M. *Crystal09*; University of Turin: Turin, Italy, 2010.

14 Frisch, M. J. et al. *Gaussian 09*, Revision A.1, Gaussian, Inc., Wallingford CT, 2009.

15 Yanai, T.; Tew, D.; Handy, N. A new hybrid exchange-correlation functional using the Coulomb-Attenuating Method (CAM-B3LYP). *Chem. Phys. Lett.* **2004**, *393*, 51–57.

16 (a) Tomasi, J; Mennucci, B.; Cammi, R. Quantum mechanical continuum solvation models. *Chem. Rev.* **2005**, *105*, 2999–3093. (b) Marenich, A. V.; Cramer, C. J.; Truhlar, D. G.; Guido, C. A.; Mennucci, B.; Scalmani, G.; Frisch, M. J. Practical computation of electronic excitation in solution: Vertical excitation model. *Chem. Sci.* **2011**, *2*, 2143–2161.

17 Dapprich, S.; Komáromi, I.; Byun, K. S.; Morokuma, K.; Frisch, M. J. A new ONIOM implementation in Gaussian 98. 1. The calculation of energies, gradients and vibrational frequencies and electric field derivatives. *J. Mol. Struct. (Theochem)* **1999**, *462*, 1–21.

18 (a) Hratchian, H. P.; Parandekar, P. V.; Raghavachari, K.; Frisch, M. J.; Vreven, T. QM:QM electronic embedding using Mulliken atomic charges: Energies and analytic gradients in an ONIOM framework. *J. Chem. Phys.* **2008**, *128*, No. 034107. (b) Jacquemin, D.; Perpète, E. A.; Laurent, A. D.; Assfeld, X.; Adamo, C. Spectral Properties of Self-Assembled Squaraine-Tetralactam: A theoretical assessment. *Phys. Chem. Chem. Phys.* **2009**, *11*, 1258–1262. (c) Le Bahers, T.; Di Tomaso, S.; Peltier, C.; Fayet, G.; Giacovazzi, R.; Tognetti, V.; Prestianni, A.; Labat, F. Acridine orange in a pumpkin-shaped macrocycle: Beyond solvent effects in the UV−visible spectra simulation of dyes. *J. Mol. Struct. (Theochem)* **2010**, *954*, 45–51.

19 Newns, D. Self-consistent model of hydrogen chemisorption. *Phys. Rev.* **1969**, *178*, 1123–1135.

20 Labat, F.; Baranek, Ph.; Domain, C.; Minot, C.; Adamo, C. Density functional theory analysis of the structural and electronic properties of TiO_2 rutile and anatasepolytypes: Performances of different exchange-correlation functionals. *J. Chem. Phys.* **2007**, *126*, No. 154703.

21 Labat, L.; Baranek, Ph.; Adamo, C Structural and electronic properties of selected rutile and anatase TiO_2 surfaces: an ab initio investigation. *J. Chem. Theory Comput.* **2008**, *4*, 341–352.

22 Labat, F.; Ciofini, I.; Adamo, C. Modeling ZnO phases using a periodic approach: From bulk to surface and beyond. *J. Chem. Phys.* **2009**, *131*, No. 044708.

23 Corà, F; Alfredsson, M.; Mallia, G.; Middlemiss, D. S.; Mackrodt, W. C.; Dovesi, R.; Orlando, R. The performance of hybrid density functionals in solid state chemistry. *Struct. Bonding (Berlin)* **2004**, *113*, 171–232.

24 Heyd, J.; Scuseria, G. Efficient hybrid density functional calculations in solids: The HS-Ernzerhof screened Coulomb hybrid functional. *J. Chem. Phys.* **2004**, *121*, 1187–1192.

25 Le Bahers, T.; Pauporté, T.; Scalmani, G.; Adamo, C.; Ciofini, I. A TD-DFT investigation of ground and excited state properties in indoline dyes used for dye-sensitized solar cells. *Phys. Chem. Chem. Phys.* **2009**, *11*, 11276–11284.

26 Guillemoles, J. F.; Barone, V.; Joubert, L.; Adamo, C. A theoretical investigation of the ground and excited states of selected Ru and Ospolypyridil molecular dyes. *J. Phys. Chem. A* **2002**, *106*, 11354–11360.

27 Rekhis, M.; Labat, F.; Ouamerali, O.; Ciofini, I.; Adamo, C. Theoretical analysis of the electronic properties of N3 derivatives. *J. Phys. Chem. A* **2008**, *111*, 13106–13111.

28 Hazebrouck, S.; Labat, F.; Lincot, D.; Adamo, C. Theoretical insights on the electronic properties of eosin Y, an organic dye for photovoltaic applications. *J. Phys. Chem. A* **2008**, *112*, 7264–7270.

29 Labat, F.; Lainé, P. P.; Ciofini, I.; Adamo, A. Spectral properties of bipyridil ligand by time dependant density functional theory. *Chem. Phys. Lett.* **2006**, *417*, 445–451.

30 Le Bahers, T.; Adamo, C.; Ciofini, I. A qualitative index of spatial extent in charge transfer excitations. *J. Chem. Theory Comput.* **2011**, *7*, 2498–2506.

31 Le Bahers, T.; Pauporté, T.; Labat, F.; Lainé, P. P.; Ciofini, I. Theoretical procedure for optimizing dye-sensitized solar cells: From electronic structure to photovoltaic efficiency. *J. Am. Chem. Soc.* **2011**, *133*, 8005–8013.

32 Labat, F.; Adamo, C. Bi-isocotinic acid on anatase (101): Insights from theory. *J. Phys. Chem. C* **2007**, *111*, 15034–15042.

33 Le Bahers, T.; Pauporté, T.; Labat, F.; Lefèvre, G.; Ciofini, I. Acetylacetone, an interesting anchoring group for ZnO-based organic-inorganic hybrid materials: A combined experimental and theoretical study. *Langmuir* **2011**, *27*, 3442–3450.

34 Le Bahers, T.; Pauporté, T.; Labat, F.; Odobel, F.; Ciofini, I. Promising anchoring groups for ZnO-based hybrid materials: A periodic DFT investigation. *Int. J. Quantum Chem.* **2012**, *112*, 2062–2071.

35 Labat, F.; Ciofini, I.; Hratchian, H. P.; Frisch, M.; Raghavachari, K.; Adamo, C. Insights into working principles of N3/TiO_2 dye-sensitized solar cells from first principles modeling. *J. Phys. Chem. C* **2011**, *115*, 4297–4306.

36 Labat, F.; Ciofini, I.; Hratchian, H. P.; Frisch, M.; Raghavachari, K.; Adamo, C. First principle modeling of eosin-loaded ZnO films: A step toward the understanding of dye-sensitized solar cells. *J. Am. Chem. Soc.* **2009**, *131*, 14290–14298.

37 Sauvé, S.; Cass, M. E.; Coia, G.; Doig, S. J.; Lauermann, I.; Pomykal, K. E.; Lewis, N. S. Dye sensitization of nanocrystalline titanium dioxide with osmium and ruthenium polypyridyl complexes. *J. Phys. Chem. B* **2000**, *104*, 6821–6836.

38 Le Bahers, T.; Labat, F.; Pauporté, T.; Ciofini, I. Effect of solvent and additives on the open-circuit voltage of ZnO-based dye-sensitized solar cells: a combined theoretical and experimental study. *Phys. Chem. Chem. Phys.* **2010**, *12*, 14710–14719.